Localized surface nucleation of magnetization reversal

Harry Suhl
Department of Physics, Mail Code 0319, 9500 Gilman Drive, University of California–San Diego, LaJolla, California 92093-0319

H. Neal Bertram[a)]
Center for Magnetic Recording Research, and Department of Electrical and Computer Engineering, Mail Code 0401, 9500 Gilman Drive, University of California–San Diego, LaJolla, California 92093-0401

(Received 31 March 1997; accepted for publication 12 September 1997)

Standard treatments of the magnetization reversal of fine particles yield a reversal mechanism that begins with nucleation of a nonuniform or uniform energy barrier state that involves virtually the entire sample volume. Accordingly, the barrier height is essentially proportional to the sample volume. Such strong volume dependence is not observed, especially in measurements of thermally activated reversal. Numerical micromagnetic analysis also shows a variety of surface reversal modes depending on the ratio of the particle size to the exchange length. An analytic model for surface nucleation is presented here for an idealized system to illustrate this phenomenon. The corresponding barrier height does not depend on sample volume, though it may depend on surface area. Any additional size dependence will arise from the finite front velocity with which the reversal propagates. An example of thermally activated reversal is given that shows ''effective'' reversal volumes that correspond to these surface reversal modes, and thus, can be much smaller than the sample volume. © *1997 American Institute of Physics.* [S0021-8979(97)03824-3]

I. INTRODUCTION

The problem of magnetization reversal for reasons of both academic interest, as well as device applications, has been studied throughout the history of magnetic materials. The magnetization curve (''$M-H$ loop'') is a classical measurement utilized to characterize magnetic materials. Theoretical models of magnetization reversal have been limited because of complexity due primarily to the long-range magnetostatic fields. In addition, for small particles where the effects of thermal fluctuations can be significant, analysis of magnetization decay rates are extremely difficult. In general, a determination, for example, of the coercivity depends not only on the applied field magnitude and direction, but also on the ambient temperature and the temporal duration of the field.

Theoretical investigations are generally formulated as follows: The total energy of the system is expressed as a functional of the (vector) magnetization field. In general, this energy functional has several local minima besides at least one global minimum. These minima are separated by barriers. Switching of the magnetization can occur either by thermal activation over the barrier between adjacent minima, or by annihilation of a minimum by an adjacent barrier as the result of the applied magnetic field reaching its coercive (or nucleation) value.

The purpose of this study is to explore the consequences of relaxing the usual boundary conditions applied when solving continuum micromagnetic or Brown's equations[1] for the nucleation of reversal field. As expanded upon below, the observed ''effective volume'' or region associated with the initiation of magnetization reversal is, typically, much smaller than the magnetic volume.[2] The boundary condition associated with continuum micromagnetics is that the magnetization surface normal derivative or the out-of-plane magnetization component vanishes. This boundary condition arises from a continuum expansion of the exchange energy. However, due to surface inhomogeneities in real materials, or even by a direct consideration of atomic exchange, this boundary condition may not be applicable. A relaxation of this boundary condition leads to more positive nucleation fields and indicates smaller effective nucleation volumes.

A calculation of the switching rate usually begins with the assumption of exponential relaxation, with the time constant derived from the Arrhenius formula for activation over a barrier.[3] For large barriers, the solution of the Fokker–Plank equation for a single spin also gives an exponential relaxation.[4] The barrier height is determined from a micromagnetic calculation: Minimization of the energy functional with respect to the vector magnetization yields the starting configuration. The vicinity of that configuration is explored by determining the second variation of the energy due to arbitrary increments in the vector magnetization. That second variation is bilinear in the increments, and, if it is positive definite (i.e., if all its eigenvalues are positive), the starting configuration is stable. The eigenvalues are functions of the applied field (among other parameters), and a nucleation field is reached when the smallest eigenvalue falls to zero. The corresponding eigenmode often gives an approximate (linearized) indication of the shape of the spatial magnetization pattern during reversal. When the smallest eigenvalue is still positive, the mode has essentially the same shape, but now it represents the variation of the magnetization in the saddle point configuration associated with the lowest positive barrier. In this second-order procedure, the height of the barrier is essentially given by the mode amplitude, which is still

a)Electronic mail: nbertram@ucsd.edu

 0021-8979/97/82(12)/6128/10/$10.00

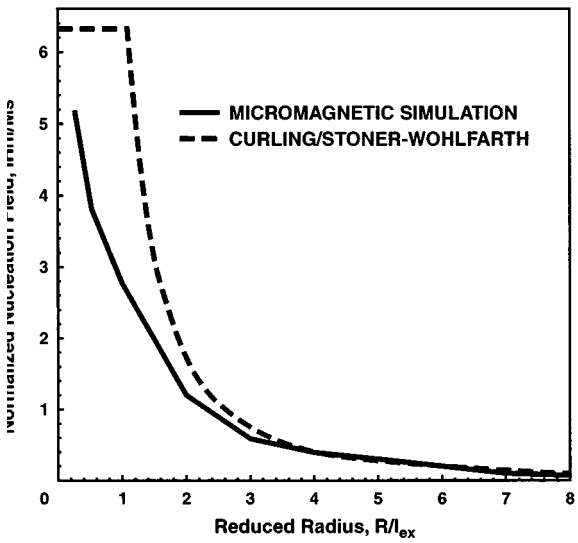

FIG. 1. Reduced nucleation field H_n/M_s vs reduced radius r/l_{ex} from micromagnetic simulation for an elongated particle. For comparison, the Stoner–Wohlfarth/curling result is shown.

arbitrary; to determine it, the fourth variation of the energy function must be calculated. In general, this procedure makes sense only for fields not too much less than the nucleation field, but in sufficiently simple cases no such differential geometry is needed. The classic example is the Stoner–Wohlfarth theory,[5] which relates to the switching of a completely uniform magnetization. The energy function is then so simple that the barrier height is immediately written down, for all applied field values. (A case almost as simple is discussed in the Appendix to this paper.)

The Stoner–Wohlfarth theory is realized in particles of dimensions significantly less than an ''exchange length,'' which (in a Heisenberg model of magnetism) is essentially equal to the lattice spacing times the square root of the exchange energy divided by a typical demagnetizing energy. In this case, the (exchange) barrier to nonuniform rotation is too large. For larger samples, nonuniform reversal modes must be considered. Reversal modes (strictly nucleation from the saturated state) initiated by curling or buckling of the magnetization field have been studied extensively. A simple rigorous treatment of the curling mode was given by Frei, Shtrikman, and Treves[6] for infinite circular cylinders. A rigorous treatment for the nucleation field for ellipsoids of revolution, in general, has also been given by Aharoni.[7]

Numerical micromagnetic analysis of the equilibrium magnetization states and reversal modes has been studied for elongated particles, both for rectangular[8–10] and ellipsoidal[11] shapes. In the case of nonellipsoidal elongated particles, such as rectangular or cylindrical shapes, the nucleation field occurs, typically, at large positive (if not infinite fields).[8,12,13] Nonetheless, the magnetization is approximately uniform before reversal. For ellipsoidal particles, the (negative) nucleation and reversal fields coincide. In Fig. 1, the numerical result for a 10:1 approximately rectangular particle is shown (crystalline anisotropy has been neglected) along with the combined Stoner–Wohlfarth/curling result. The essential scaled parameter is radius r to exchange length $l_{ex} = \sqrt{A}/M_s$. The particle was discretized into cubes of side 21_{ex}; finer discretization was shown not to alter the results. For $r/l_{ex} \ll 1$, the Stoner–Wohlfarth uniform rotation field is reached. However, as the radius is increased, there is a monotonic decrease of reversal field. At $r = l_{ex}$, the Stoner–Wohlfarth approximately intersects that for curling and the numerical result is about one-half of this value. At approximately $r = 3l_{ex}$, the numerical result comes close to that for curling, although curling is an exact eigenmode only for ellipsoids of revolution.

In numerical studies, it is difficult to precisely determine the small-angle nucleation eigenmodes, however, general patterns may be deduced. For approximately $r < 1.5l_{ex}$, the reversal mode involves a large magnetization rotation at the particle ends with subsequent ''domain-wall'' motion along the particle length to complete reversal. The reversal volume in these cases is less than the total volume, and it has been shown that application of a reversal field to only an ''effective'' volume at the particle end results in approximately the same nucleation field and mode.[8] (For the case of $r = l_{ex}$, typical of magnetic tape particles, the effective volume is approximately the cube of the diameter.) In particular relevance to the focus of this paper, numerical studies of thermally induced particle reversal[14] show a similar thermally induced reversal mode. In fact, application of thermal fluctuations solely to the ends of the particle yields the same magnetization decay time as application to the entire volume.

For larger radii, approximately, $r > 1.5l_{ex}$, the reversal processes becomes progressively nonuniform. The (large-angle) reversal process is dominated by vortex formation at the surfaces along the particle length with reversal by vortex propagation across the particle width. Thus, in this regime, the ''effective'' volume appears to be a localized surface dominated mode, roughly independent of the particle size. Numerical studies of thermal reversal of these larger particles have not yet been performed. The results shown in Fig. 1 are hardly changed if the cubic discretization is used to roughly approximate a cylinder of revolution: a $10 \times 10 \times 50$ array (a 5:1 particle) with $r = l_{ex}$ was utilized for this comparison. In addition, the reversal field is independent of the particle length, except for $r \ll l_{ex}$. For shorter particles, where the particle length is approximately the exchange length, the particle will switch by the somewhat ellipticity dependent uniform rotation nucleation field.[10]

Numerical micromagnetic analysis of the reversal field of a well-discretized ellipsoid of revolution of 4.615 ellipticity has been solved by a finite element technique.[15] The dependence of the nucleation (reversal) field with r/l_{ex} follows that of Stoner–Wohlfarth/curling reasonably well. This result is expected since nucleation by curling has been shown to be a lower bound for elliposids,[16] and the numerical analysis utilized the boundary conditions given by Brown.[1] Although effective reversal volumes have not been determined for ellipsoids, reversal patterns indicate[15] for $r \approx l_{ex}$ that at magnetization deviations somewhat beyond the initial nucleation, reversal is predominately at the particle center where the largest cross-section diameter occurs. For $r \gg l_{ex}$, the (large-angle) reversal mode is by surface-induced vortex formation

and propagation across the width of the particle,[15] similar to rectangular particles.[8] The conclusion from numerical studies is that the ''effective'' volumes of particle reversal can be less than the particle volume in agreement with experimental results.[2,17]

In this paper, we present a model calculation in which the barrier is shown to be confined to a thin layer at the surface; consequently, activation energies for switching are at best only weakly dependent on sample volume. A plane surface bounding a semi-infinite half-space filled with magnetic material is considered. Uniaxial anisotropy with easy axis normal to the surface is assumed, and the material in its lowest state is uniformly magnetized by a sufficiently strong magnetic field normal to the face. A neighboring stationary state of slightly higher energy is derived by solving the micromagnetic equations in the form of a linear integrodifferential equation. The boundary conditions are not restricted as in Brown's analysis;[1] thus, the magnetization normal to the surface or the normal derivative of the magnetization are not required to vanish at the surface. This equation is solved by Wiener–Hopf–Hilbert methods in Fourier space.[18,19] In addition, a rigorous solution, not confined to the vicinity of the ground state, is derived for a restricted case in the Appendix, and it confirms the conclusions of the linearized analysis. Although this analysis is strictly applicable only to the idealized geometry, it is expected to be useful as a guide to nucleation configurations in particles of dimensions well in excess of an exchange length. One may ask why these ''surface states'' have been missed in previous analytic treatments. The reason is that these treatments have invariably imposed homogeneous boundary conditions on the magnetization fields (such as vanishing of the normal derivative at the boundary). It is argued here (by an example) that these conditions are unduly restrictive. Any type of inhomogeneity in the boundary conditions allows for modes confined to the surface.

The outline of this paper is as follows: In Sec. II, a general discussion of stationary states for a magnetic system is presented. In Sec. III, application is made to a semi-infinite space with field normal to the surface. In Sec. IV, discussion is given of these results in terms of the typical spin-wave spectrum as well as an application to a field parallel to a surface. In the Appendix, a direct calculation is presented that checks the validity of the perturbative approach taken in Secs. II and III.

II. THEORY OF STATIONARY STATES

Of all possible magnetization vector fields $\mathbf{M}(\mathbf{x})$, the most important ones are those that make the total magnetic energy E insensitive to a small variation $\delta\mathbf{M}(\mathbf{x})$ of $\mathbf{M}(\mathbf{x})$, to first order in the small deviation, so that δE is zero to that order. The vector field $\mathbf{M}(\mathbf{x})$ is then said to be in a stationary state. If the change $\delta^2 E$ calculated to second order in $\delta\mathbf{M}(\mathbf{x})$ is positive definite (i.e., positive for all possible variations $\delta\mathbf{M}(\mathbf{x})$, then the corresponding $\mathbf{M}(\mathbf{x})$ that made δE vanish represents a stable magnetic configuration. If there is a $\delta\mathbf{M}(\mathbf{x})$ that makes $\delta^2 E$ vanish, the configuration is marginally stable, and a small change in the appropriate parameter then causes the magnetization to switch. That particular form of $\delta\mathbf{M}(\mathbf{x})$ also gives a rough (linearized) indication of the shape of the switching mode.

The total energy of the system is

$$E(\mathbf{M})=\int d^3x\Bigg[2l_{\mathrm{ex}}^2(\nabla\mathbf{M})^2-\mathbf{H}\cdot\mathbf{M}(\mathbf{x})+K(\mathbf{M}(\mathbf{x}))+\int d^3x'\Bigg\{\frac{\mathbf{M}(\mathbf{x})\cdot\mathbf{M}(\mathbf{x}')}{|\mathbf{x}-\mathbf{x}'|^3}-3\frac{\mathbf{M}(x)\cdot(\mathbf{x}-\mathbf{x}')\mathbf{M}(x')\cdot(\mathbf{x}-\mathbf{x}')}{|\mathbf{x}-\mathbf{x}'|^5}\Bigg\}\Bigg], \tag{1}$$

where $l_{\mathrm{ex}}=\sqrt{A}/M_s$, the exchange length, is a dimensionless measure of the exchange energy. K is the crystalline anisotropy energy, and $\mathbf{H}$ is a uniform applied field. Stationary states are found by extremizing this energy with respect to $\mathbf{M}(\mathbf{x})$, subject to the constraint that $(\mathbf{M}(x))^2$ must be independent of position and equal to the square of the saturation magnetization M_s. Introducing the Lagrange parameter field $\lambda(\mathbf{x})$ and extremizing $E+1/2\int d^3x\lambda(\mathbf{x})(\mathbf{M}(\mathbf{x}))^2$, the stationary condition is

$$\delta E(\mathbf{M})-\int d^3x\lambda(\mathbf{x})\mathbf{M}(\mathbf{x})\cdot\delta\mathbf{M}(\mathbf{x})=0, \tag{2}$$

where

$$\delta E(\mathbf{M})=\int_{\mathrm{sample}} d^3x d\mathbf{M}(\mathbf{x})\cdot\Bigg[-2l_{\mathrm{ex}}^2\nabla^2\mathbf{M}(\mathbf{x})+\int_{\mathrm{sample}} d^3x'\Bigg\{\frac{(\mathbf{M}(\mathbf{x}')}{|\mathbf{x}-\mathbf{x}'|^3}-3\frac{[\mathbf{M}(\mathbf{x})\cdot(\mathbf{x}-\mathbf{x}')](\mathbf{x}-\mathbf{x}')}{|\mathbf{x}-\mathbf{x}'|^5}\Bigg\}-\mathbf{H}+\frac{\partial K(\mathbf{M}(\mathbf{x}))}{\partial\mathbf{M}(\mathbf{x})}\Bigg]+2l_{\mathrm{ex}}^2\int_{\mathrm{surface}} d\mathbf{M}(\mathbf{x})\cdot(d\mathbf{S}\cdot\nabla)\mathbf{M}(\mathbf{x}). \tag{3}$$

The surface integral, which may also be written as $\int_{\mathrm{surface}}\delta\mathbf{M}(\mathbf{x})\cdot d\mathbf{M}(\mathbf{x})/dn/dS$, where dn is an element of normal, arises from the familiar partial integration of the incremented exchange term. If Eq. (2) is to hold for arbitrary $\delta\mathbf{M}(\mathbf{x})$, the coefficients of $\delta\mathbf{M}(\mathbf{x})$ in both the surface and volume integrals must vanish at each point. Thus, the normal derivative of $\mathbf{M}$ must vanish on the surface, so that

$$\lambda(\mathbf{x})\mathbf{M}(\mathbf{x})=(\delta E)_{\mathrm{vol}}/\delta\mathbf{M}(\mathbf{x}), \tag{4}$$

where

$$(\delta E)_{\mathrm{vol}}/\delta\mathbf{M}(\mathbf{x})=-2l_{\mathrm{ex}}^2\nabla^2\mathbf{M}(\mathbf{x})+\int_{\mathrm{sample}} d^3x'\Bigg\{\frac{(\mathbf{M}(\mathbf{x}')}{|\mathbf{x}-\mathbf{x}'|^3}-3\frac{[\mathbf{M}(\mathbf{x}')\cdot(\mathbf{x}-\mathbf{x}')](\mathbf{x}-\mathbf{x}')}{|\mathbf{x}-\mathbf{x}'|^5}\Bigg\}-\mathbf{H}+\frac{\partial K(\mathbf{M}(\mathbf{x}))}{\partial\mathbf{M}(\mathbf{x})}. \tag{5}$$

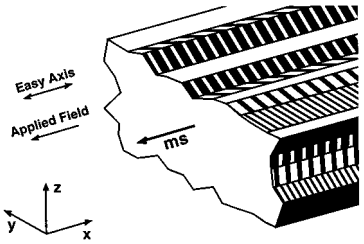

FIG. 2. Illustration of the semi-infinite space of analysis. The plane is defined by the y, z axis. The surface of this space is at $x=0$ and positive x denotes the distance into the magnetic material. The easy axis for the crystalline anisotropy is along the x direction and the applied field H, and the initial saturated magnetization M_s is directed out of the surface (along negative x).

(Actually, as explained below, the notion of the vanishing normal derivative is not quite correct, and comes from an incorrect limiting process for the surface energy.)

Remembering that the square of the magnetization vector is constant everywhere, it follows that

$$[\lambda(\mathbf{x})]^2 M_s^2 = [(\delta E)_{\mathrm{vol}}/\delta \mathbf{M}(x)]^2, \tag{6}$$

and, therefore,

$$\frac{\mathbf{M}(\mathbf{x})}{M_S} = -\frac{(\delta E)_{\mathrm{vol}}/\delta \mathbf{M}(\mathbf{x})}{|(\delta E)_{\mathrm{vol}}/\delta \mathbf{M}(\mathbf{x})|}. \tag{7}$$

We now specialize the problem to the simplest geometry that illustrates the point of this paper. The magnetic medium occupies the half-space to the right of an infinite boundary plane $x=0$ (Fig. 2). The applied magnetic field is normal to that plane, as is the anisotropy axis of a uniaxial anisotropy energy $K(\mathbf{M}) = -KM_x^2/M_s^2$; both these energies favor alignment of the magnetization normal to the plane. For a sufficiently large applied field, a stationary state that satisfies Eq. (7), as well as the boundary condition, is then $(M_s,0,0)$. To find its stability properties conveniently, we expand around the stationary state (7) to first order in the deviation (equivalent to finding $\delta^2 E$). We write $\mathbf{M}(x) = (M_s - o(\mathbf{m}^2), \mathbf{m}(\mathbf{x}))$, where $\mathbf{m}(\mathbf{x})$ is a small two-component vector in the plane normal to the x axis. Then, to lowest order in this deviation, all quantities in the numerator of Eq. (7) are transverse, and the denominator gives no first-order contributions at all, so that it must be evaluated for a saturated magnetization. In that state, the dipolar contribution is equal to

$$M_s \int_{\mathrm{sample}} d^3\mathbf{x}' \left\{ \frac{1}{|\mathbf{x}-\mathbf{x}'|^3} - 3\frac{(x-x')^2}{|\mathbf{x}-\mathbf{x}'|^5} \right\}. \tag{8}$$

Equation (8) is the demagnetizing field for the magnetization saturated and normal to the film plane, and is equal to $4\pi M_s$. The condition (7) for marginal stability can, thus, be written

$$\{(H_{\mathrm{tot}}/M_s) - 2l_{\mathrm{ex}}^2 \nabla^2\}\mathbf{m}(\mathbf{x}) = -\int_{\mathrm{sample}} d^3x' \left\{ \frac{\mathbf{m}(\mathbf{x}')}{|\mathbf{x}-\mathbf{x}'|^3} - 3\frac{(\mathbf{x}_T - \mathbf{x}_T')(\mathbf{m}(\mathbf{x}')\cdot(\mathbf{x}-\mathbf{x}'))}{|\mathbf{x}-\mathbf{x}'|^5} \right\}, \tag{9a}$$

$$H_{\mathrm{tot}} = H + 2K/M_s - 4\pi M_s, \tag{9b}$$

is the total field seen inside the sample in the continuum limit. Equation (9a) is meaningful only if the point $\mathbf{x}$ lies within the sample. If the sample were infinite rather than semi-infinite, the equation would be trivially solved in terms of Fourier transforms. It would yield the permissible spatial periodicities of extended states, as well as conditions under which no real periods exist. For the infinite case, Eq. (9) in wave-number space yields

$$(H_{\mathrm{tot}}/M_s + 2l_{\mathrm{ex}}^2\mathbf{k}^2)\mathbf{m}_k = -4\pi \mathbf{k}_T(\mathbf{k}_T\cdot\mathbf{m}_k)/\mathbf{k}^2, \tag{10}$$

where $\mathbf{k}_T$ denotes the transverse part of $\mathbf{k}$. Elimination of the two components of $\mathbf{m}_k$ gives two possibilities,

$$H_{\mathrm{tot}}/M_s + 2l_{\mathrm{ex}}^2\mathbf{k}^2 + 4\pi\mathbf{k}_T^2/\mathbf{k}^2 = 0 \tag{11a}$$

and

$$(H_{\mathrm{tot}}/M_s + 2l_{\mathrm{ex}}^2\mathbf{k}^2) = 0. \tag{11b}$$

Equations (11a) and (11b) correspond to zero-frequency modes of the spin-wave spectrum as discussed in Sec. IV. If H_{tot} is positive, not all the wave numbers in Eqs. (11a) and (11b) can be real, thus, there must be localized states; for imaginary k, the Fourier transform e^{ikx} becomes the localized form $e^{-|k|x}$. Fully extended states exist only for negative H_{tot}, that is, for

$$H < H_{\mathrm{demag}} - 2K/M_s, (=4\pi M_s - 2K/M_s, \quad \text{in the present geometry}), \tag{12}$$

where $H_{\mathrm{demag}} - 2K/M_s$ is the nucleation field for uniform rotation. Thus, if the surface is regarded as an ''imperfection,'' for fields before nucleation ($H_{\mathrm{tot}}>0$), a localized stationary state of limited range, decaying exponentially away from the surface, can occur. In the following section, the existence of localized states is established rigorously.

A. Discussion of boundary conditions

A spatially localized state, with exponential decay from the surface, does not exist if the condition is imposed that the normal derivative of the magnetization at the surface vanishes. As an illustration, consider the differential equation $y'' + \kappa^2 y = 0$ for positive κ^2. The solution is a linear superposition of $e^{\pm i\kappa x}$. If the ''normal derivative'' dy/dx is to vanish at $x=0$, the only nontrivial (non-null) solution must involve *both* these waves. On the other hand, if κ^2 is negative, only one solution, $\propto e^{-x\sqrt{-\kappa^2}}$, is acceptable for large x. Then, if the condition $y'(0)=0$ is imposed, only the null solution is possible. The same will be true for *any* homogeneous linear boundary condition. However, the requirement of a vanishing normal derivative in the present case is not strictly correct. As a simple example, consider a linear chain

of exchange-coupled discrete spins in a magnetic field. The energy per cross-sectional area may be written as

$$E_A=\sum_{i=1}^{N}\left\{\frac{2JS^2}{a^2}\cos\left(\frac{M_{i+1}-M_i}{M_s}\right)+HM_ia\right\}, \tag{13}$$

where J is the atomic exchange constant and a is the lattice constant. Minimization of this expression with respect to the interior spins gives the usual result in the continuum limit. However, minimization with respect to the end spin M_1, and normalization by aM_s gives

$$\left(\frac{2JS^2}{a^3M_s^2}\right)\sin\left(\frac{M_2-M_1}{M_s}\right)+H=0, \tag{14}$$

or, in the continuum limit,

$$\left.\frac{l_{\rm ex}^2\,dM}{a\,dx}\right|_{x=0}+H=0, \tag{15}$$

where $l_{\rm ex}^2=A/M_s^2$ and $A=2JS^2/a$.[20] Equation (15) is homogeneous only in the limit of zero field, though it is small for fields small compared with the exchange field. A similar conclusion holds if the surface spin is exchange coupled to some strongly pinned, essentially immobile, impurity spin. We shall suppose that surface conditions are sufficiently complex so that an inhomogeneous boundary condition is appropriate even in zero field.

III. THE SEMI-INFINITE CASE

In this section, we specifically analyze Eq. (9a) for the geometry shown in Fig. 2, where the field is normal to the semi-infinite surface. Equations (5) and (9a), of course, apply only inside the medium or for the region $x>0$. However, the expression on the right-hand side of Eq. (9a) represents the total dipolar field generated by the transverse magnetization increment and applies for all x both inside and outside the medium. The difficulty of solving Eq. (9a), in its present form, is due to the fact that in a half-space, the Fourier transform method fails. The problem is basically of the Wiener–Hopf type,[19] except that the kernel of the integral does not have the necessary analyticity properties required by that method. However, using Hilbert's method,[18] a solution may be obtained as follows.

A. Definition of auxiliary function

We first define a function that covers the entire space for $-\infty<x<+\infty$. This function is comprised of the sum of $\mathbf{m}_+(x)$ and $\mathbf{m}_-(x)$. $\mathbf{m}_+(x)$ is defined only for the region of $x>0$ and is identical to the magnetization inside the medium; $\mathbf{m}_+(x)$ vanishes for $x<0$:

$$\mathbf{m}_+(x)=\mathbf{m}(x),\quad x>0$$
$$=0,\quad x<0, \tag{16a}$$

$\mathbf{m}_-(x)$ is an auxiliary (unphysical) function that is defined for the region

$$\mathbf{m}_-(x)\neq 0,\quad x<0$$
$$=0,\quad x>0, \tag{16b}$$

TABLE I. Eigenvalues and eigenvectors of the Fourier transformed energy minimization expression. Note: θ_k is the angle between the wave vector and the x axis.

Eigenvalues	Normalized eigenvector
$D_1=1$	$\mathbf{v}_t=(-k_z,k_y)/k_T$
$D_2=1+(4\pi\sin^2\theta_k/C)$	$\mathbf{v}_l=(k_y,k_z)/k_T$

which is zero for $x>0$. The Fourier transforms of these functions are given by

$$\mathbf{m}_+(\mathbf{k})=\int_0^\infty dx e^{ik_xx}\int\int d^2x_T e^{i\mathbf{k}_T\cdot\mathbf{x}_T}\mathbf{m}_+(\mathbf{x}), \tag{17a}$$

and

$$\mathbf{m}_-(\mathbf{k})=\int_{-\infty}^0 dx e^{ik_xx}\int\int d^2x_T e^{i\mathbf{k}_T\cdot\mathbf{x}_T}\mathbf{m}_-(\mathbf{x}). \tag{17b}$$

By extending k_x into the complex plane, it is seen that the first of these functions is analytic in the entire upper half k_x plane, while the second is analytic in the entire lower half k_x plane.

The stability equation that results from the vanishing of Eq. (5) yields, in terms of these new functions,

$$\{(H_{\rm tot}/M_s)+2l_{\rm ex}^2\nabla^2\}\{\mathbf{m}_+(\mathbf{x})-\mathbf{m}_-(\mathbf{x})\}$$
$$=-\int_{\rm all/space}d^3x'\left\{\frac{\mathbf{m}(\mathbf{x}')}{|\mathbf{x}-\mathbf{x}'|^3}\right.$$
$$\left.-3\frac{(\mathbf{x}_T-\mathbf{x}_T')(\mathbf{m}(\mathbf{x}')\cdot(\mathbf{x}-\mathbf{x}')}{|\mathbf{x}-\mathbf{x}'|^5}\right\}. \tag{18}$$

Equation (18) applies over the entire three-dimensional space. Fourier transforms techniques may now be utilized and, in fact, the Fourier transform of Eq. (18) is:

$$\{(H_{\rm tot}/M_s)+2l_{\rm ex}^2k^2\}\{\mathbf{m}_+(\mathbf{k})-\mathbf{m}_-(\mathbf{k})\}$$
$$=4\pi\mathbf{k}_T[\mathbf{k}_T\cdot\mathbf{m}_+(\mathbf{k})]/k^2. \tag{19}$$

Equation (19) can be written as a matrix equation

$$B\mathbf{m}_+=\mathbf{m}_-, \tag{20}$$

where

$$B=\begin{pmatrix}(1+4\pi k_y^2/Ck^2), & 4\pi k_yk_z/Ck^2\\ 4\pi k_yk_z/Ck^2 & (1+4\pi k_z^2/Ck^2)\end{pmatrix}, \tag{21a}$$

with

$$C=(H_{\rm tot}/M_S+2l_{\rm ex}^2k^2). \tag{21b}$$

The eigenvalues and eigenvectors of B are given in Table I. The Fourier transforms $\mathbf{m}_+(\mathbf{k})$ and $\mathbf{m}_-(\mathbf{k})$ may be expanded in terms of these eigenvectors:

$$\mathbf{m}_+=\mathbf{v}_tn_+^{(1)}+\mathbf{v}_ln_+^{(2)}\quad \mathbf{m}_-=\mathbf{v}_tn_-^{(1)}+\mathbf{v}_ln_-^{(2)}. \tag{22}$$

Substitution of Eq. (22) into Eq. (20) yields the two equations

$$D_1n_+^{(1)}=n_-^{(1)}, \tag{23a}$$

$$D_2n_+^{(2)}=n_-^{(2)}. \tag{23b}$$

For the expansion coefficients $n_{\pm}^{(1,2)} \cdot \mathbf{n}_{\pm}$ may be regarded as boundary values just above and just below the real k_x axis of a single vector function $\mathbf{n}(k_x)$ of the complex variable k_x. Taking logarithms of both sides of Eqs. (23a) and (23b) gives

$$\ln n_{+}^{(1,2)} - \ln n_{-}^{(1,2)} = -\ln D_{1,2}. \tag{24}$$

The eigenvalues D_1, D_2 satisfy the Hölder condition on the real k_x axis (at least for fields above nucleation), in that the maximum variation is bounded for both D_1 and D_2. The Hilbert method[15] may be utilized and, thus, Eq. (24) is satisfied if

$$\ln n_{+}^{(1,2)}(k_x, \mathbf{k}_T) = -\frac{1}{2\pi i} \int_{-\infty}^{\infty} dk_x' \frac{\ln D_{1,2}(k_x', \mathbf{k}_T)}{k_x' - k_x - i\epsilon} + P(k_x, \mathbf{k}_T), \tag{25}$$

or

$$n_{+}^{(1,2)}(\mathbf{k}) = |D_{1,2}|^{-1/2} e^{1/2\pi i\, p \int_{-\infty}^{\infty} dk' \frac{\ln D_{1,2}(k_x', \mathbf{k}_T)}{k_x - k_x'} + P(\mathbf{k})}, \tag{26}$$

where $P(k)$ is an arbitrary polynomial.

However, this simple solution fails to meet the boundary condition at infinite k_z. There, the transverse magnetization components must go to zero, by the Riemann–Lebesgue lemma. On the other hand, expression (26) remains finite there, even if the polynomial is taken to be zero. (This conclusion is also found in Miskhelishvili,[19] p. 91.) To examine this dilemma, we consider the mode with the eigenvalue equal to unity. The corresponding eigenvector is $\mathbf{m}_{+} \propto (-k_z, k_y)$ and it is purely transverse to $\mathbf{k}_T$. [By contrast, the other eigenstate is purely longitudinal: $\mathbf{m} \propto (k_y, k_z)$.] Therefore, Eq. (10) simplifies drastically: the dipolar field does not appear in the transversely polarized state. In this case, it is possible to simply solve the differential equation

$$\left\{ (H_{\text{tot}}/M_s) + 2l_{\text{ex}}^2 \left(-\mathbf{k}_T^2 + \frac{\partial^2}{\partial x^2} \right) \right\} \mathbf{m} = 0, \quad \mathbf{m} \cdot \mathbf{k}_T = 0, \tag{27}$$

subject to $\mathbf{m}$ taking on a given value at $x=0$. Of the two exponential solutions, for the positive total field, we chose the one tending to zero at infinity. Thus, the initial amplitude drives the entire solution. More generally, the energy density may be supplemented with a linear functional of $\mathbf{m}$. The coefficient function of this term then acts as an inhomogeneous term on the right-hand side of the above differential (27). Thus, the more usual solution in which only the amplitude at $x=0$ is specified, is a special case. If that amplitude (or the coefficient function in the general case) is zero, the problem has only the trivial null solution.

The same considerations apply to the discussion of $n^{(2)}$. Unless an inhomogeneous term is added, the only solution vanishing at infinite wave number is the null solution. So, we must add to the integral on the right-hand side of Eq. (9) a term $-\mathbf{g}(\mathbf{x}) \cdot \mathbf{m}(\mathbf{x})$. If we wish, we may chose a $\mathbf{g}(\mathbf{x})$ localized near $x=0$ to parallel the usual procedure of specifying the amplitude only at $x=0$ for the state discussed in the previous paragraph. For example, the boundary condition given by Eq. (15) could be written in the form of a suitable $\mathbf{g}(\mathbf{x})$. In this case, it is necessary to solve the inhomogeneous Hilbert problem,

$$B\mathbf{m}_{+} = \mathbf{m}_{-} + \mathbf{f}(\mathbf{k}), \tag{28}$$

where $\mathbf{f}(\mathbf{k}) = \mathbf{g}(\mathbf{k})/C$. [$C$ is defined in Eq. (21b).] Expanding $\mathbf{f}$ in eigenvectors,

$$\mathbf{f} = \mathbf{v}_t\, f^{(1)} + \mathbf{v}_l\, f^{(2)}, \tag{29}$$

yields the two equations

$$D_1 n_{+}^{(1)} = n_{-}^{(1)} + f^{(1)}, \tag{30a}$$

$$D_2 n_{+}^{(2)} = n_{-}^{(2)} + f^{(2)}, \tag{30b}$$

where D_1 and D_2 are given in Table I.

The essential point of the discussion is made by considering Eq. (30b) first. Let X_{+}^{h}, X_{-}^{h} denote the solution of the homogeneous equation for $n_{\pm}^{(2)}$ (30b). In this case,

$$D_2 = \frac{X_{-}^{(h)}}{X_{+}^{h}}, \tag{31}$$

so that Eq. (30b) becomes

$$\frac{n_{+}^{(2)}}{X_{+}^{h}} - \frac{n_{-}^{(2)}}{X_{-}^{h}} = \frac{f^{(2)}}{X_{h}^{-}}, \tag{32}$$

from which it follows that at a given, fixed $\mathbf{k}_T$,

$$n_{+}^{(2)}(k_x) = \frac{1}{2\pi i} X_{+}^{h}(k_x) \int_{-\infty}^{\infty} dk_x' \frac{f^{(2)}(k_x')}{X_{h}^{-}(k_x')(k_x' - k_x - i\epsilon)}. \tag{33}$$

The dependence in Eq. (33) on the transverse k vector is implied, but not shown. The solution given by Eq. (33) properly vanishes as $k_x \to \infty$, provided $\mathbf{g}(k_x) \to 0$ as $k_x \to \infty$.

The solutions X_{+}^{h}, X_{-}^{h} can be identified with the solution of the homogeneous (15). However, it is simpler to proceed by utilizing the so-called ''factorization'' method[16] as follows: For positive total field, D_2 has no real zeroes and, thus, we may write

$$D_2 = \frac{(k_x - q_1)(k_x - q_1^*)(k_x - q_2)(k_x - q_2^*)}{(k_x + ik_T)(k_x - ik_T)(k_x + ia)(k_x - i\alpha)}, \tag{34}$$

where

$$a = \sqrt{\frac{H_{\text{tot}}}{4l_{\text{ex}}^2} + k_T^2}, \tag{35}$$

and the q's are the roots of

$$(k_x^2 + k_T^2)\{(H_{\text{tot}}/M_s) + Jl^2(k_x^2 + k_T^2)\} + 4\pi k_T^2 = 0, \tag{36}$$

choosing q_1, q_2 to be in the upper half-plane. Thus, Eq. (31) may be written in the form

$$X_{+}^{h} \frac{(k_x - q_1^*)(k_x - q_2^*)}{(k_x + ik_T)(k_x + ia)} = X_{-}^{h} \frac{(k_x - ia)(k_x - ik_T)}{(k_x - q_1)(k_x - q_2)}. \tag{37}$$

The form of Eq. (37) is such that the left-hand side is analytic in the upper half-plane and the right-hand side is analytic in the lower half-plane. Since the two sides are equal, they are both equal to a function without any singularities in

the finite part of the plane. This function must be a constant, if the solution to Eq. (33) is to vanish at infinity. Thus, from Eq. (33),

$$n_+^{(2)}(k_z)=\frac{1}{2\pi i}\frac{(k_x+ik_T)(k_x+ia)}{(k_x-q_1^*)(k_x-q_2^*)} \times\int_{-\infty}^{\infty}dk_x'\,\frac{(k_x'-ik_T)(k_x'-ia)f^{(2)}(k_x')}{(k_x'-q_1)(k_x'-q_2)(k_x'-k_x-i\epsilon)}. \tag{38}$$

The longitudinal part of the physical $\mathbf{m}(\mathbf{x})$ is the inverse Fourier transform

$$m_l(x)=\int_{-\infty}^{\infty}d^3k e^{-i\mathbf{k}\cdot\mathbf{x}}n_+^{(2)}(\mathbf{k}). \tag{39}$$

The k_x integral, at given $\mathbf{k}_T$, may be evaluated by contour integration, with the contour closed in the lower half-plane. The remaining k_x' integral cannot be so evaluated, because of the generally unknown analyticity properties of $g(k_x')$. Denoting the integral in Eq. (38) by $I(k_x)$, the result for the longitudinal part of $\mathbf{m}$ is

$$m_l(x)=-e^{-iq_1^*x}\frac{(q_1^*+ik_T)(q_1^*+ia)I(q_1^*)}{q_1^*-q_2^*} -e^{-iq_2^*x}\frac{(q_2^*+ik_T)(q_2^*+ia)I(q_2^*)}{q_2^*-q_1^*} -\int_{-\infty}^{\infty}dk_x^*\,\frac{k_x'^2(k_x'^2+a^2)f^{(2)}(k_x')e^{-ik_x'x}}{(k_x'-q_1)(k_x'-q_2)(k_x'-q_1^*)(k_x'-q_2^*)}. \tag{40}$$

Thus, the solution consists of two decaying exponentials, together with a term that, for general g, does not necessarily decrease exponentially. For a highly localized driving term, g is practically constant, so that $f^{(2)}=\text{const}/C$. In that case, evaluation of the integral becomes possible, and yields terms that decrease exponentially exactly like the first two terms in Eq. (40), plus an additional decaying term arising from the complex zero of C located in the lower half-plane. Note that the denominators of the first two terms of Eq. (40) are proportional to $1/\sqrt{l_{\text{ex}}^2k_T^2-H_{\text{tot}}}$. However, the resulting infinity is integrable, so that this singularity has no special significance in the calculation of the inverse Fourier transform.

The other stationary state corresponding to D_1 is very much simpler. Since $D_1=1$, it follows that $X_+^h=X_-^h$, and since D_1, of course, has no poles or zeroes, we may chose both X's equal to unity. Then, we simply have

$$n_+^{(1)}-n_-^{(1)}=f^{(1)}=g^{(1)}/C, \tag{41}$$

so that

$$n_+^{(1)}=\int_{-\infty}^{\infty}dk_x'\,\frac{g^{(1)}(k_x')}{[(H_{\text{tot}}/M_s)+2l_{\text{ex}}^2k_x'^2+k_T^2](k_x'-k_x-i\epsilon)}. \tag{42}$$

Taking the inverse Fourier transform gives the transverse part of the physical m at given transverse vector $\mathbf{k}_T$:

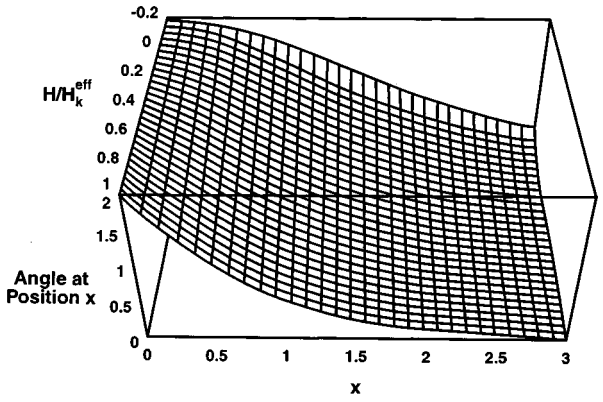

FIG. 3. Spatial variation of magnetization angle vs distance from the surface for a variety of normalized effective fields (H/H_k^{eff}).

$$m(x,\mathbf{k}_T)=\int_{-\infty}^{\infty}dk_x'\,\frac{g^{(1)}(k_x';\mathbf{k}_T)e^{-ixk_x'}}{[H_{\text{tot}}/M_s+2l_{\text{ex}}^2(k_x'^2+k_T^2)]}. \tag{43}$$

This is exactly the same result that would have been obtained, had dipolar effects been neglected and the usual second-order differential equation with exchange only had been solved. Evidently, when the total field is positive, evaluation of this integral gives, at fixed $\mathbf{k}_T$, exponential decay for all reasonable forms of $g^{(1)}$.

In Fig. 3, the spatial variation of the magnetization is plotted for the surface stationary states corresponding to a range of normalized total fields. The actual curves come from the analysis in the Appendix. However, the results are illustrative of the general theory presented here. The field is plotted as H/H_k^{eff}, where $H_k^{\text{eff}}=H_k-2\pi M_s$ is the sum of crystalline and (thin-film) shape anisotropy. The angular variation of the magnetization decreases with distance from the surface as expected. Note that as the field is decreased and approaches the nucleation field for uniform rotation, the spatial decay occurs over a progressively extended distance. Nucleation of the uniform mode occurs at $H=-H_k^{\text{eff}}$ and at that value the magnetization deviation would extend uniformly throughout the sample.

IV. DISCUSSION

In the previous sections, nonuniform excitations of the magnetization have been considered. The ''classic'' nonuniform magnetization small-angle excitation for an infinitely large sample is the spin-wave spectrum.[21] The results presented in this work are related to the spin-wave modes. The excitation frequency of a spin wave with wave-number $\mathbf{k}$ when precession is taken into account is

$$\omega_k=\gamma\sqrt{(H+H_K+Dk^2)(H+H_K+Dk^2+4\pi\,\sin^2\,\theta_k)}, \tag{44}$$

where D represents the exchange energy. The two terms in Eq. (44) correspond to waves perpendicular ($\theta_k=0°$) and parallel ($\theta_k=90°$) to the applied field direction. A finite frequency corresponds to a stationary state with a positive second variation of the system energy. Nucleation occurs when the second variation vanishes, or equivalently, a zero-

frequency mode first occurs.[1] In this simple case, corresponding to uniform excitation ($k=0$), the nucleation field occurs at the Stoner–Wohlfarth value of $H=-H_k$. For fields before nucleation $H>-H_k$, nucleation can occur only for complex values of k_x, e.g.,

$$m_x(k)\propto e^{ikx}\propto e^{-x\sqrt{(H+H_k)/D}}. \tag{45}$$

Thus, the results in this paper can be viewed as localized zero-frequency excitations. For a finite-size sample of spherical shape, the solely magnetostatic modes have been solved.[21] This analysis did not include the exchange energy, but a somewhat similar discrete spectrum will also occur for the long-wavelength portion of the complete spin-wave spectrum. For large samples (radius greater than the exchange length), the solution[21] is probably a good approximation to the long-wavelength spin-wave spectrum. Nonetheless, there is a lowest-frequency mode (at a finite k) that vanishes at nucleation ($\omega=0$). At fields above this nucleation field, complex wave numbers will yield a vanishing frequency and, again, localized modes will occur.

In numerical micromagnetic simulations of the reversal of axially magnetized, elongated particles, as discussed in the introduction, it is found for large particles that switching moves inward from the long sides.[8,11] The corresponding ideal geometry is the semi-infinite plane, magnetized parallel to the surface. Although the methods of the preceding sections can be applied to this case also, it is simpler to adapt the curling solution for infinite longitudinally magnetized cylinders,[6] and to discard the requirement of the vanishing derivative normal to the surface (see the discussion of boundary conditions at the end of Sec. II). A variational analysis to the energy minimization of Eq. (5) in cylindrical coordinates has the form of a Bessel function of the first kind:

$$m_\phi\propto J_1(\mu r)e^{ikz}, \tag{46}$$

which describes the variation of the azimuthal component m_ϕ as a function of radius r and distance z along the cylinder axis, where, in our present notation,

$$\mu=\sqrt{-k^2-(HM_s+K)/2(M_s l_{\rm ex})^2}. \tag{47}$$

Curling (and, presumably switching) begins at the least negative value of the field that satisfies $J_1'(\mu)=0$. When the field has not reached that negative value, and an inhomogeneous boundary condition is admitted, then there is a corresponding solution that involves only a surface magnetization fluctuation, and has the form:

$$m_\phi\propto I_1(r\sqrt{k^2+(HM_s+K)/2(M_s l_{\rm ex})^2})e^{ikz}, \tag{48}$$

where I_1 is the first-order Bessel function of imaginary argument [note that the surface is at $r=1$, so that Eq. (48) entails decay of magnetization rotation from the surface to the center at $r=0$]. If the cylinder radius is much larger than an exchange length, the energy in this state is evidently very much lower than the energy of a curling state pervading the entire volume. We expect that solutions of this form for various values of k are the seeds of corresponding numbers of vortices (for sample length L, the number is $n\approx Lk/\pi$) forming at the sidewall of the cylinder.

V. CONCLUSIONS

We have shown that inhomogeneous boundary conditions will lead to barrier states of the magnetization field near the surface of ferromagnetic samples. The energy of a barrier state is proportional to the surface area times the penetration depth of the state, and for samples exceeding the penetration depth, this energy is obviously less than that of the barrier states filling the entire volume, which are calculated with homogeneous boundary conditions. However, as the applied field gets very close to the coercive field calculated on the basis of homogeneous boundary conditions, the penetration depth becomes large (equal to the entire sample dimensions), and then there is not much difference between the two conditions. Well below that nominal coercive field, however, the barrier for inhomogeneous boundary conditions is much lower, explaining the observed high thermal activation rates.

ACKNOWLEDGMENT

This work is supported by the National Science Foundation, Grant No. NSF/DMR-9400439.

APPENDIX

To check the viability of our approximate procedure, we derive the result in a particular case, nonperturbatively, without recourse to the series expansion of the magnetization. Consider again the semi-infinite medium, initially magnetized normal to the surface, with zero transverse components of the magnetization. The magnetization fluctuation will be presumed to correspond to a rotation angle that varies in a direction normal to the surface only (corresponding to the case of a ''buckling mode,'' with $k_T=0$ in the linearized analysis). This is a possible switching mode that involves dipolar forces in the simple form of a shape anisotropy that adds to the effective uniaxial anisotropy. In terms of $\theta(x)$, the rotation angle of the magnetization vector away from the field, the local dipolar energy is simply $2\pi M_s^2\cos^2\theta(x)$. The energy per unit area can then be written

$$E\propto\int_0^\infty dx\left\{l_{\rm ex}^2M_s^2\left(\frac{d\theta}{dx}\right)^2-HM_s\cos\theta-K^{\rm eff}\cos^2\theta\right\}, \tag{A1}$$

where $K^{\rm eff}=K-2\pi M_s^2$. The extrema of Eq. (A1) satisfy the differential equation

$$\frac{d^2\theta}{dx^2}-h\sin\theta-q\sin\theta\cos\theta=0, \tag{A2}$$

where

$$h=H/(2l_{\rm ex}^2M_s),\quad q=K^{\rm eff}/(l_{\rm ex}^2M_s^2), \tag{A3a}$$

and, in scaled form,

$$\frac{h}{q}=\frac{H}{H_k-4\pi M_s}=\frac{H}{H_k^{\rm eff}}. \tag{A3b}$$

A first integral of Eq. (A2) is

$$\left(\frac{d\theta}{dx}\right)^2+2h\cos\theta+q\cos^2\theta=\text{const}. \tag{A4a}$$

For a surface-localized state, we require a solution for which both θ and θ' go to zero as x goes to infinity. This means that

$$\left(\frac{d\theta}{dx}\right)^2 = 2h(1-\cos\,\theta)+q\,\sin^2\,\theta$$

$$= 4\{h+q\,\cos^2(\theta/2)\}\sin^2(\theta/2). \tag{A4b}$$

For positive h, the solution decays to zero from any assigned value θ_0 at $x=0$. For negative h of magnitude less than q, this solution exists only for θ_0 sufficiently small so that $\cos^2(\theta_0/2)>|h|/q$. If the initial angle fails to meet this condition, the angle oscillates with x between two limits, and we have only a buckling state, pervading the whole sample. In that case, the constant (call it C) in Eq. (A4a) must be chosen so that

$$\cos^2\,\theta+\frac{2h}{q}\cos\,\theta-\frac{C}{q}=0, \tag{A5}$$

has two real roots for θ, and the angle oscillates between the two.

Writing $t=\tan(\theta/2)$ in Eq. (A4a), and choosing the negative square root, gives

$$\frac{dt}{dx}=-t\sqrt{ht^2+(h+q)}. \tag{A6}$$

For $h+2q>0$, this can be integrated to give

$$e^{-\sqrt{(h+q)}x}=\left(\frac{\tan\,\frac{1}{2}\theta}{\tan\,\frac{1}{2}\theta_0}\right)\cdot\frac{1+\sqrt{1+\kappa\,\tan^2\,\frac{1}{2}\theta_0}}{1+\sqrt{1+\kappa\,\tan^2\,\frac{1}{2}\theta}}, \tag{A7}$$

where $\kappa=h/(h+q)$. The substitution $\sqrt{\kappa}\tan\frac{1}{2}\theta=\sinh\psi$ renders Eq. (A7) into the simple form $\tanh\frac{1}{2}\psi=e^{-\sqrt{h+q}x}\tanh\frac{1}{2}\psi_0$. Reexpressed in terms of θ, Eq. (A7) becomes

$$\tan\,\tfrac{1}{2}\theta=\kappa^{-1/2}\sinh\,\psi$$

$$=\kappa^{-1/2}\frac{2e^{-\sqrt{h+q}x}\tanh(\frac{1}{2}\sinh^{-1}[\sqrt{\kappa}\tan\,\frac{1}{2}\theta_0])}{1-e^{-2\sqrt{h+q}x}\tanh^2(\frac{1}{2}\sinh^{-1}[\sqrt{\kappa}\tan\,\frac{1}{2}\theta_0])}. \tag{A8}$$

Here, θ_0 is the deviation from saturation at $x=0$. Note that this solution correctly has $\theta\to 0$ as $x\to\infty$. Provided $|h|<q$, this result remains real and holds, as well, for negative h (i.e., imaginary κ). Equation (A8) is valid up to a maximum initial value

$$\theta_0=\theta_{\rm crit}=2\,\arccos\sqrt{|h|/q}, \tag{A9}$$

beyond which buckling occurs and depends on $|h|/q$.

Figure 3 shows θ versus x for $\theta_{\rm crit}=114.59°$, for various values of $|h|/q$ [or utilizing Eq. (A3b), the variable h/q is shown as $H/H_k^{\rm eff}$]. The critical value of h/q is then -0.2919. For a small initial angle and a correspondingly wide range of values of $|h|/q$, the decay is essentially exponential, as indicated by the linearized theory.

To find the energy per unit area, it is convenient to choose θ as an integration variable rather than x, via the substitution $dx\to d\theta/(d\theta/dx)$, which is permissible for initial angles less than the critical value. The energy deviates from the (saturated) ground state (by the amount):

$$\Delta E=l_{\rm ex}^2M_s^2\int_0^{\theta_0}d\theta\,\frac{2h(1-2\,\cos\,\theta)-q\,\cos 2\theta-(-2h-q\})}{\sqrt{2h(1-\cos\,\theta)+q\,\sin^2\,\theta}}$$

$$=l_{\rm ex}^2M_s^2\int_0^{\theta_0}d\theta\,\frac{4h(1-\cos\,\theta)+q(1-\cos 2\theta)}{\sqrt{2h(1-\cos\,\theta)+q\,\sin^2\,\theta}}$$

$$=8l_{\rm ex}^2M_s^2\int_0^{\theta_0}d\theta\,\sin(\theta/2)\sqrt{h+q\,\cos^2(\theta/2)}\,. \tag{A10}$$

This integration can be performed and equals

$$\Delta E=8_{\rm ex}^2M_s^2\sqrt{q}\left\{\sqrt{\frac{h}{q}+1}-\sqrt{\frac{h}{q}+\cos^2\,\frac{\theta_0}{2}}\right.$$

$$\left.+\frac{h}{q}\ln\frac{\sqrt{h/q+1}+1}{\sqrt{h/q+\cos^2\,(\theta_0/2)}+\cos^2\,(\theta_0/2)}\right\}. \tag{A11}$$

Contours of equal ΔE as a function of h/q and of initial angle θ_0 are shown in Fig. 4. To the left of the boundary curve $(h/q)+\cos^2(\theta_0/2)=0$, buckling occurs.

For *small* values of the deviation, this model is adequately mimicked by expanding the trigonometric functions in Eq. (A2) up to cubic terms, which yields

$$\theta''-(h+q)\,\theta+(h/6+q/2)\,\theta^3=0. \tag{A12}$$

The critical value of θ_0 is then

$$\theta_{\rm crit}=\sqrt{2\frac{h+q}{\frac{1}{3}h+q}}\cong\sqrt{3(1-|h|/q)}, \tag{A13}$$

provided h is only slightly larger than $-q$. For larger values of the deviation, the cubic term dominates and Eq. (A9) holds. The solution of Eq. (A12) then oscillates between two limits, yielding the buckling state. A rough estimate of the

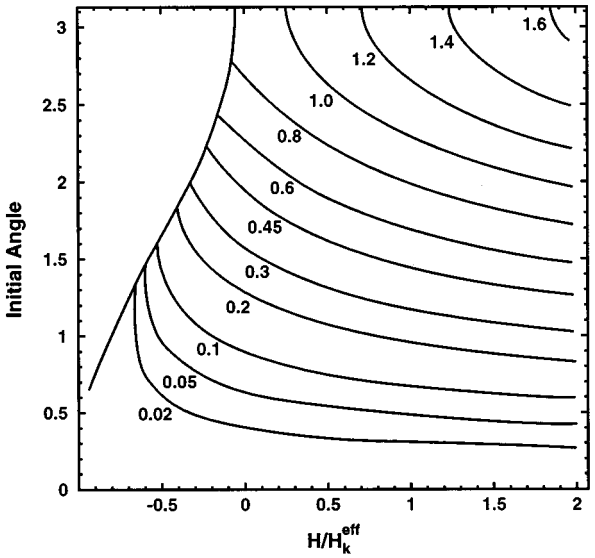

FIG. 4. Lines of equal barrier height plotted for the variation of initial magnetization angle and normalized net magnetic field ($H/H_k^{\rm eff}$).

period of the buckling rate may be made by writing $\theta = \theta_{\text{crit}} + \mu$ (47). For small values of μ, the linearized version of Eq. (A12) gives a spatial buckling frequency equal to $\sqrt{2(q-|h|)}$.

[1] W. F. Brown, Jr., *Micromagnetics* (Interscience, New York, 1963).
[2] F. Li and R. M. Metzger, IEEE Trans. Magn. **33**, 3715 (1997).
[3] L. Néel, in *Progress in Low Temperature Physics*, Vol. 1, edited by C. J. Gorter (North-Holland, Amsterdam, 1995), p. 336.
[4] W. F. Brown, Jr., IEEE Trans. Magn. **5**, 1196 (1979).
[5] E. Stoner and E. P. Wohlfarth, Philos. Trans. R. Soc. London, Ser. A **240**, 74 (1948).
[6] E. H. Frei, S. Shtrikman, and D. Treves, Phys. Rev. **106**, 446 (1957).
[7] A. Aharoni, Phys. Status Solidi **16**, 1 (1966).
[8] M. E. Schabes, J. Magn. Magn. Mater. **95**, 249 (1991).
[9] M. E. Schabes and H. N. Bertram, J. Appl. Phys. **64**, 5832 (1988).
[10] C. Seberino and H. N. Bertram, IEEE Trans. Magn. **33**, 3055 (1997).
[11] B. Yang and D. R. Fredkin, J. Appl. Phys. **79**, 5755 (1996).
[12] W. Chen, Ph.D thesis, University of California–San Diego, 1992.
[13] A. Holz, Phys. Status Solidi **25**, 576 (1968).
[14] E. Boerner and H. N. Bertram, IEEE Trans. Magn. **33**, 3052 (1997).
[15] B. Yang, Ph.D. thesis, University of California–San Diego, 1997.
[16] A. Aharoni, J. Phys.: Condens. Matter (to be published).
[17] M. P. Sharrock, IEEE Trans. Magn. **26**, 193 (1990).
[18] B. Nobel, *Methods Based on the Wiener–Hopf Technique for the Solution of Partial Differential Equations* (Pergamon, New York, 1958).
[19] N. I. Muskhelishvili, *Singular Integral Equations* (Dover, New York, 1992).
[20] C. Kittel, Rev. Mod. Phys. **21**, 541 (1949).
[21] L. R. Walker, in *Magnetism*, edited by G. T. Rado and H. Suhl (Academic, New York and London, 1963), Chap. 8.